Table 1
Total Number of BCGs and Those Hosting AGN in Each Redshift Bin

Redshift Bin	AGN-hosting BCG	All BCG
0.00–0.39	0	141
0.39–0.55	3	142
0.55–0.71	7	143
0.71–1.30	12	137

3.2. Calculating the AGN fraction

We compute the fraction of galaxy clusters with AGN-hosting BCGs based on the number of BCGs whose mid-IR colors are redder than expected, as described in Section 3.1.1, in four redshift bins to study the redshift evolution. With the probability estimated in Section 2.2, we first include in Figure 3 all the BCGs that are identified with a probability that is higher than 20%, meaning that some clusters will have more than one BCG candidate. The fraction of AGN-hosting BCGs is calculated over the total number of BCG candidates, instead of over the total number of clusters in each bin. We discuss these particular choices of calculating AGN-hosting BCG fraction in Section 4. The bins are defined from $z = 0$–1.3 in such a way that each bin contains roughly the same number of BCG candidates ($\sim$140 BCGs; see Table 1 for the exact number). This choice of binning yields uniform counting statistics across all redshifts. The uncertainties associated with the AGN fractions are estimated from the Wilson interval, which remains accurate for fractions near 0 and 1 (Brown et al. 2001).

4. Results and Verification

Table 1 shows the number of AGN-hosting BCG in the four redshift bins, whereas the blue points in Figure 6 show the fraction of AGN-hosting BCGs in the four bins with their corresponding 68% confidence intervals. We observe that the fraction is increasing with redshift in the SPT sample. Gray crosses show the fraction of points that have residuals lower than -0.2. If the scatter is truly random, there should be a similar number of points below -0.2 compared to those above +0.2, which are classified as AGNs. This result implies that the increasing trend of the AGN-hosting BCGs fraction is not a result of the data quality. Such a trend has been suggested and shown in previous works (e.g., Hlavacek-Larrondo et al. 2013; McDonald et al. 2016; Bîrzan et al. 2017; Gupta et al. 2020; Mo et al. 2020). In particular, we show that the fraction is $\sim$2% at $z \approx 0.5$, which is consistent with what Somboonpanyakul et al. (2021a) found from studying extreme central BCGs in clusters. We note that because some AGN-dominated galaxies will have poor photometric redshift constraints as they are estimated from the stellar spectrum and not from the power-law spectrum of the AGN, we might misidentify these galaxies in our BCG-finding algorithm. This implies that the number of BCGs with central AGNs found in this work gives a lower limit for the AGN-hosting BCG fraction, and the actual evolution could be even stronger.

One way to evaluate the observed result with the chosen bins is to perform Fisher's Exact Test in order to see whether there are any associations between two categorical variables. The result shows that we can reject the null hypothesis of independence with P-value = 0.00045, meaning that there is a statistically significant association (>99.9%) between redshift and whether or not BCGs host AGNs.

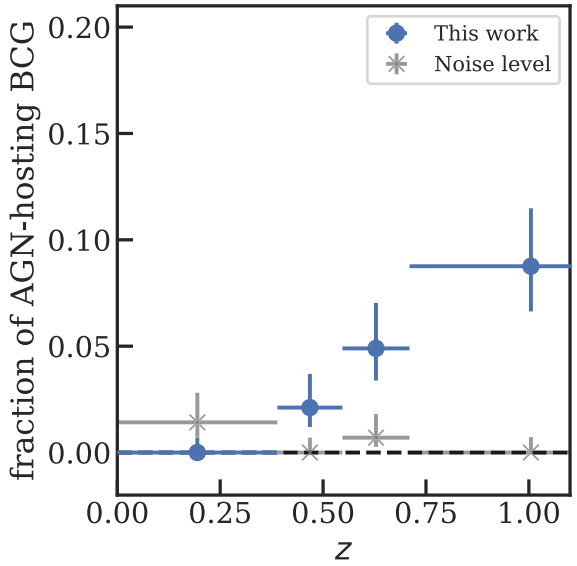

Figure 6. The fractions of AGN-hosting BCGs as a function of redshift. Blue points show the fractions from this work, which come from the $W1$–$W2$ color residual in the SPT sample. The size of the error bar takes the binomial uncertainty into account. Gray crosses show the fraction of points that has residuals lower than −0.2, which we consider a "noise level." This figure demonstrates that the fraction of AGN-hosting BCG increases with redshift.

The approaches taken in this work are as follows: (i) we include all BCG candidates with a probability higher than 20% in our sample instead of picking only one BCG per cluster, and (ii) we calculate the fraction of BCGs with AGNs over the total number of BCG candidates, and not the fraction of clusters with AGN-hosting BCGs over the total number of clusters. The reason for these two assumptions is that we want to include AGN-hosting BCGs from systems with more than one obvious BCG, which are typical for merging systems such as the Coma cluster (Zwicky 1933), and the Bullet cluster (Markevitch et al. 2004). We perform consistency checks to address both of these assumptions. Figure 7 shows the fraction of AGN-hosting BCGs when we consider the most likely BCG candidates, every BCG candidate with a probability higher than 20%, and every BCG candidate with a probability higher than 10%. This figure shows that the increasing trend of the fraction of AGN-hosting BCGs over redshift remains consistent in all three scenarios, regardless of how we select BCGs.

On the other hand, Figure 8 shows the results when we use different definitions of AGN fractions. The gray and blue points in Figure 8 are calculated with the total number of clusters as a denominator instead of the number of BCG candidates. For the blue points, we consider one BCG per cluster and include both the probability of being BCGs, as calculated in Section 2.2, and the uncertainty of the mid-IR color for each BCG to emphasize the fact that the uncertainties of identifying BCGs and BCG colors are higher at high redshift. The empty gray dots are the largest possible fractions, which are calculated from clusters for which any of their potential BCGs are considered as AGNs, while the empty gray squares are the smallest possible fractions by counting only clusters for which all of their BCG candidates are classified as AGNs. This figure illustrates that all of these definitions qualitatively give the same conclusion as our initial results.

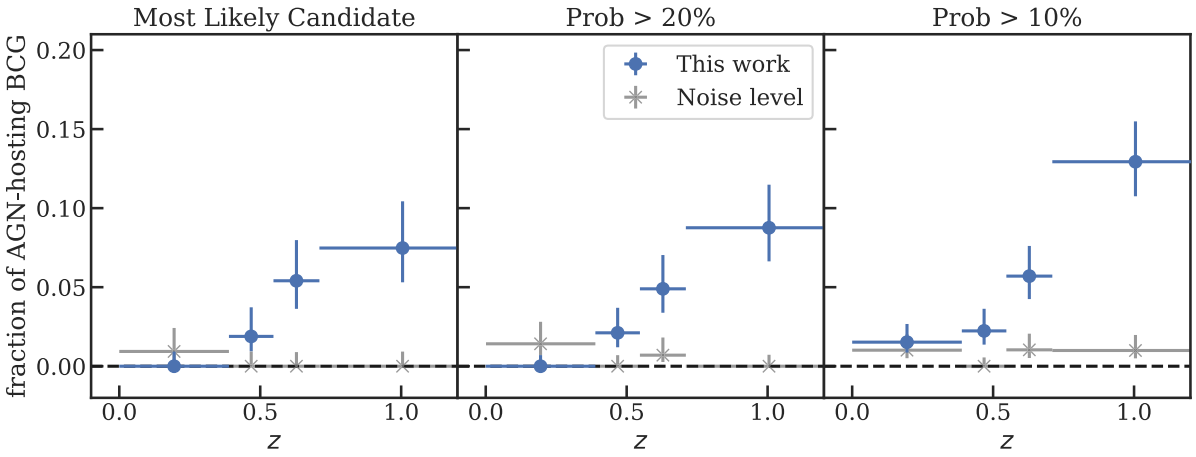

Figure 7. All three panels show the fractions of AGN-hosting BCGs, similar to Figure 6. The left panel (triangles) shows the fraction when we consider only the most likely BCG for each cluster. The middle panel (dots) includes all possible BCGs with a probability higher than 20%, while the right panel (squares) includes those with a probability higher than 10%. In all scenarios, the fraction increases as a function of redshift.

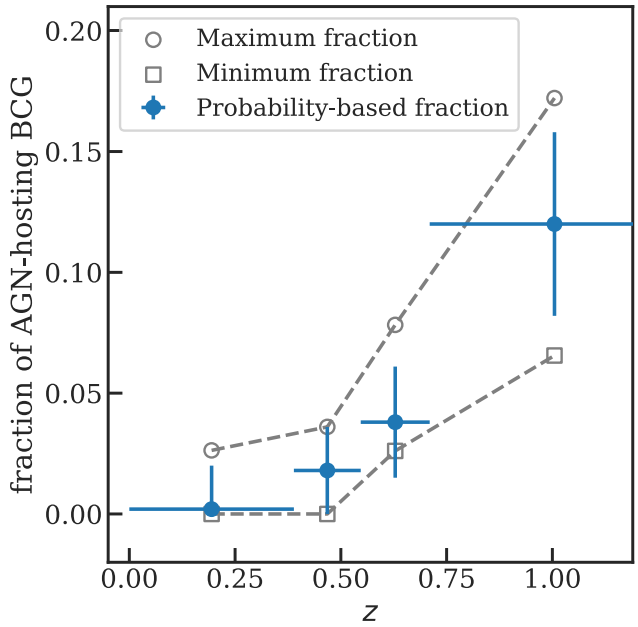

Figure 8. The fractions of clusters with AGN-hosting BCGs, similar to Figure 6. The blue points assume one BCG per cluster and incorporate the probability of being a BCG, estimated from Section 2.2. The empty gray dots are for clusters for which any of their potential BCGs are considered as AGNs, which is equivalent to the maximum fraction. The empty gray squares only include clusters whose BCG candidates are all considered AGNs, which is the minimum fraction. This figure shows that all of these definitions qualitatively give the same conclusion as our initial results.

We compare our results with the AGN fraction in field galaxies to determine whether there is a difference in the fractions between the two environments. The green and pink squares in the left panel of Figure 9 show the field X-ray AGN fractions from the zCOSMOS survey (Silverman et al. 2009) and the Chandra Multiwavelength Project results (ChaMP; Haggard et al. 2010), respectively. The results from our work are consistent with these two results, suggesting that the source of fuel required for AGN accretion in field galaxies could be similar to that in the brightest cluster galaxies. Additional evidence for the AGN fraction evolution in field galaxies has been seen in other works. For example, Lehmer et al. (2007) reported an evolution in early-type galaxies ($z \sim 0.7$) consistent with the $(1+z)^3$ pure luminosity evolution model. The dotted gray line in Figure 9 shows the curve for $(1+z)^3$, although it is only intended to be illustrative because it is arbitrarily normalized. The dashed line instead shows the curve for $(1+z)^{5.3}$. This line was first suggested by Martini et al. (2009), who showed that the AGN fraction of cluster members increases as $\sim(1+z)^{5.3}$ for AGN with an X-ray luminosity higher than $L_x > 10^{43}$ erg s^{-1}, hosted by luminous galaxies. We also fit the power-law model ($\propto(1+z)^{\alpha}$) to the blue points in Figure 9 and find a power-law exponent $\alpha = 4.1 \pm 1.0$, as shown by the dash-dotted brwon line, which is consistent with the results from both Lehmer et al. (2007) and Martini et al. (2009). Nevertheless, there are caveats regarding the relation between cluster BCGs and field galaxies. One concern is that the AGN selection criteria for both BCGs and field galaxies are different, making it difficult to make a direct comparison between the two. In addition, according to the work about the evolution of AGN luminosity, which shows that AGNs in galaxies tend to be brighter at high redshift (Hasinger et al. 2005; Silverman et al. 2008), we would naturally expect to find a higher AGN fraction at high redshift because we usually selected AGNs based on a certain luminosity threshold.

5. Discussion

The results obtained in Section 4 demonstrate that given a single-burst stellar population model, there is an increase in the fraction of AGN-hosting BCGs with redshift. This finding is consistent with previously published studies (e.g., Hlavacek-Larrondo et al. 2013; Bîrzan et al. 2017), which focused on different samples with distinct selection effects. In particular, the results from Hlavacek-Larrondo et al. (2013) and ours, as shown in the middle panel of Figure 9, show the same trend of an increasing fraction of AGN-hosting BCGs with redshift. However, the normalizations are vastly different. Hlavacek-Larrondo et al. (2013) claimed that the fraction of active BCGs is 30% at $z \approx 0.1$ and 60% at $z \approx 0.5$. On the other hand, we show that the fraction is smaller than 20% at all redshift bins. A possible explanation stems from the very different samples that these works consider. While this study is based on an effectively mass-selected sample of clusters, without any consideration of X-ray properties, the sample used by Hlavacek-Larrondo et al. (2013) focused solely on highly

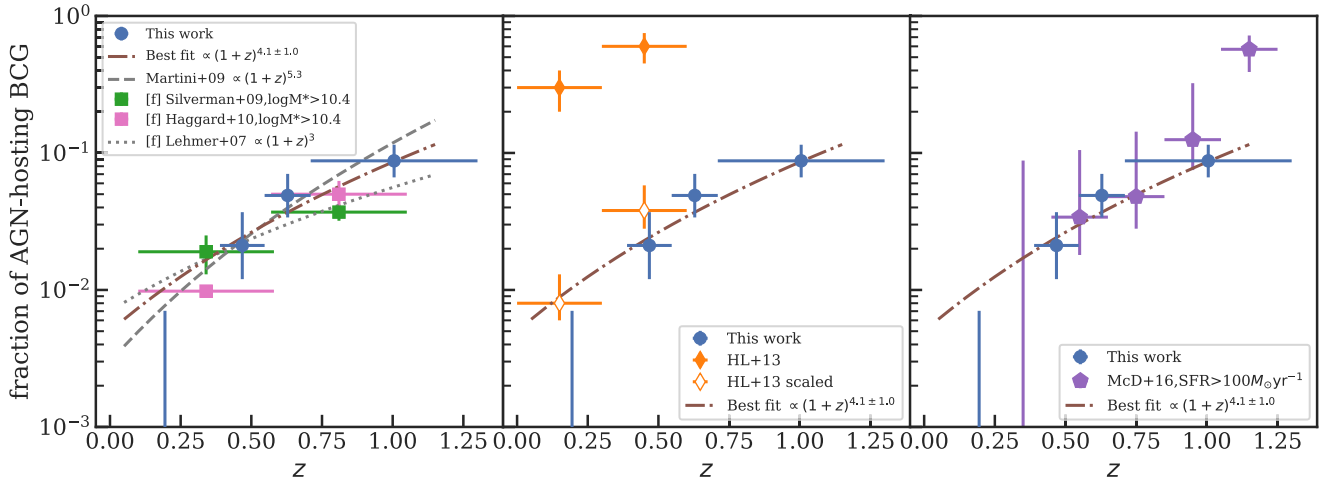

Figure 9. Comparison of the fraction of clusters with AGN-hosting BCGs to other published works. Left: Green and pink squares are the field AGN fraction from Silverman et al. (2009) and Haggard et al. (2010), respectively. The dotted gray line indicates pure luminosity evolution $\propto (1+z)^3$ as suggested by Lehmer et al. (2007), while the dashed gray line shows the $(1+z)^{5.3}$ line suggested by Martini et al. (2009). The dash-dotted brown line displays the best-fit model in the form $(1+z)^{4.1\pm1.0}$. Middle: Orange diamonds show the estimated fractions of BCGs with bright AGNs ($\log_{10}(L_{\rm X,nuc}$ [erg s^{-1}]) > 42.2) from Hlavacek-Larrondo et al. (2013), and open orange diamond showing the scaled version by changing the total number of clusters to the larger parent sample that Hlavacek-Larrondo et al. (2013) had drawn from because this work only focuses on highly X-ray luminous clusters ($L_{\rm X} > 3\times10^{44}$ erg s^{-1}). Right: Purple points show the fraction of BCGs with an SFR $> 100\,M_\odot$ yr^{-1} from McDonald et al. (2016).

X-ray luminous clusters ($L_{\rm X,cluster} > 3\times10^{44}$ erg s^{-1}), which show clear X-ray cavities. To place these two studies on the same scale, we modify the denominator used by Hlavacek-Larrondo et al. (2013) in calculating the AGN fraction to account for the full parent population of clusters from which their sample of 32 clusters was drawn. Given that this previous work included a subsample of clusters drawn from the REFLEX (Böhringer et al. 2004), eBCS (Ebeling et al. 2000), MACS (Ebeling et al. 2001), and SPT-XVP (McDonald et al. 2013) surveys, we consider these surveys in their entirety as the total population (the denominator) when calculating the AGN fraction. With this rescaling, we find that the fraction of BCGs hosting powerful AGN is consistent between our work and Hlavacek-Larrondo et al. (2013), and that the observed evolution is consistent in the two studies. We note that AGN are identified in very different ways in these two samples, but they both select at the extreme end—the few most mechanically powerful and the most IR-bright outbursts. The fact that these two works agree after the aforementioned rescaling is applied is reassuring, although a much more thorough analysis (and proper bias correction) is needed before conclusions about the coevolution of jet power and mid-IR emission can be made.

An increase in the fraction of BCGs hosting central AGNs with redshift suggests that the accretion rates of the SMBHs in the BCGs are higher at high redshift because the AGN luminosity is proportional to the accretion rate. Several works about the relation between the mean black hole accretion rates and the cavity (kinetic)/quasar (radiative) power of the central AGN (Churazov et al. 2005; Russell et al. 2013) have shown that as black hole accretion increases in the BCGs, the cavity power of the AGN also increases to counteract the cooling from the accretion in the form of a negative feedback cycle. However, as the black hole accretion rates rise to near the Eddington limit, the cavity/jet power seems to be saturated, and the radiative power tends to dominate at this level of accretion. The fact that the radiative power from AGNs usually promotes more cooling in the ICM instead of preventing it suggests that a well-regulated feedback system between the central black hole and its host cluster is no longer possible at high accretion, implying that some galaxies might not have a fully established AGN feedback loop at this redshift range.

A similar conclusion has been reached in the work related to star-forming galaxies (Webb et al. 2015; McDonald et al. 2016; Bonaventura et al. 2017), which showed that the fraction of starburst BCGs is higher at high redshift ($z > 1$). Specifically, McDonald et al. (2016) found the fraction of BCGs with SFR over $10\,M_\odot$ yr^{-1} to be $34\pm5\%$ at $0.25 < z < 1.25$, compared to $\sim$1%–5% at $z\sim0$. The right panel of Figure 9 compares the fraction of AGN-hosting BCGs in this work with the fraction of starburst BCGs ($\rm SFR_{BCG} > 100\,M_\odot\,yr^{-1}$) from McDonald et al. (2016), demonstrating that in the center of cluster environments, both massive starburst galaxies and bright AGNs behave similarly. These two results strongly indicate that AGN feedback might not be as effective to prevent overcooling at high redshift as we have previously thought.

All of these results lead us to suspect that the reason for the observed redshift trend and the breakdown of AGN feedback at high redshift comes from the fact that there is an abundance of cold gas at that redshift. In the local universe, BCGs typically grow by merging with gas-poor satellites without triggering any AGN activity. However, BCGs at high redshift could grow by merging with gas-rich members instead. Cold gas from the mergers could be a source of fuel for increasing AGN activities in the center of clusters. This is consistent with the picture we obtain from the studies of starburst BCGs (Webb et al. 2015; McDonald et al. 2016) because cold dense clouds from gas-rich mergers could provide enough matter required for creating new stars. Further evidence supporting a gas-rich merger explanation includes the prevalence of cluster galaxies with massive CO or cold gas reservoirs at high redshift (Noble et al. 2017, 2019; Hayashi et al. 2018; Markov et al. 2020) and the detections of molecular gas in many BCGs (Dunne et al. 2021). This scenario can also explain recent studies about the cool-core (CC) fraction, which shows no sign of evolution over the same redshift range (McDonald et al. 2017; Ruppin et al. 2021). If AGN feedback breaks down at high redshift, one

would expect that the CC fractions of clusters would be higher because more gas should have been cooled near the center. However, if black hole accretion and star formation in high-redshift BCGs are fueled by something other than cooling of the hot gas, such as gas-rich mergers (Barnes & Hernquist 1991; Hopkins et al. 2006), it would be reasonable to think that the trends of AGN- and starburst-hosting BCG fractions would be different from the trend of the CC fraction. If this observed increase in AGN activity is linked to gas-rich mergers rather than ICM cooling, we would expect to see an increase in scatter in the $P_{\rm cav}$ versus $L_{\rm cool}$ relation (Rafferty et al. 2006) at $z > 1$.

Another possible scenario to explain the trend of high AGN-hosting BCG fraction at high redshift has to do with cluster mergers. It has been shown both in simulations (Fakhouri et al. 2010) and observations (McDonald et al. 2017) that the cluster merger rate is significantly higher at high redshift. Major mergers between two clusters have the potential of disrupting a tightly regulated AGN feedback loop and promote black hole accretion and star formation by potentially increasing the local turbulence of the system. This is consistent with the turbulent picture in the precipitation model for AGN feedback, called "chaotic cold accretion (CCA)," which states that turbulence is a key component in driving nonlinear thermal instability and extended condensation (Voit et al. 2015; Gaspari et al. 2020). Turbulent forcing can help stimulate precipitation and condensation by increasing the velocity dispersion of the ambient medium, resulting in more black hole accretion and star formation (Voit 2018). With a more energetic environment in the early universe, it is reasonable to assume that the turbulence will be higher at high redshift, resulting in higher black hole accretion rates. The recent discovery of CHIPS $1911+4455$, a merging galaxy cluster with a massive starburst at the center, provides strong evidence that mergers can indeed increase star formation (Somboonpanyakul et al. 2021a, 2021b). With the development of next-generation X-ray observatories such as Athena and Lynx, we will be able to directly measure motions in the hot gas and determine whether mergers of groups/clusters can boost cooling via an increase in turbulence.

Last, Figure 5 shows that the BCG of the Phoenix cluster remains the most extreme AGN in the entire SPT-SZ sample, which covers a 2500 $\deg^2$ area and spans all redshifts. In combination with the recent work from the CHiPS survey (Somboonpanyakul et al. 2021a), which confirmed that the Phoenix cluster hosts the most extreme BCG with the strongest CC at $z < 0.7$, the runaway cooling phase, as we have seen in the Phoenix cluster, is indeed extremely rare.

6. Conclusion

In this work, we present results for the mid-IR colors of BCGs in SPT-selected galaxy clusters at $0 < z < 1.3$. This study allows us to track the evolution of BCG properties over $\sim$9 Gyr of cluster growth. In particular, we focus our work on black hole accretion in BCGs, which turns these central galaxies into bright AGNs. Our findings are summarized as follows:

1. Assuming a single-burst stellar population model, we find statistically significant evidence ($> 99.9\%$) for a mid-IR excess in high-redshift BCGs compared to low-redshift BCGs, suggesting an increase with redshift in the fraction of AGN-hosting BCGs in galaxy clusters over $0 < z < 1.3$. For the lower-redshift bins ($z < 0.6$), an increase is not statistically significant, and the results are compatible with the noise level. On the other hand, we see an increase in the fraction of BCGs with AGNs in high-redshift bins ($z > 0.6$), similar to what others have found in previous works (Hlavacek-Larrondo et al. 2013; McDonald et al. 2016; Bîrzan et al. 2017).
2. We show that our results are consistent with both the evolution of the fraction of AGNs in field galaxies (Silverman et al. 2009; Haggard et al. 2010) and the fraction of starburst BCGs (Webb et al. 2015; McDonald et al. 2016), suggesting that the reason for the evolution of both AGN and starburst fraction could come from the fact that more cold gas is available in the early universe. This should lead to a higher level of gas-rich mergers in BCGs, which could fuel both AGN activity and star formation at the center of clusters. Some caveats about the direct comparison between cluster and field galaxies remain and range from selection criteria to the evolution of AGN luminosity.
3. Another possible explanation for the increase in the fraction of AGN-hosting BCGs with redshift could be a higher level of local turbulence from dynamically active galaxy clusters at high redshift, leading to elevated cooling and subsequent black hole accretion. However, for this scenario, it is difficult to explain the similarity to the trends in field galaxies.
4. We do not see any additional cluster with a BCG that is as extreme in the mid-IR color as the Phoenix cluster. In other words, the Phoenix cluster likely hosts the most extreme central AGN in the SPT sample.

An enhancement of AGN activity in BCGs at high redshift compared to low redshift, which is similar in magnitude to the increase observed in field galaxies and cluster members, suggests that this increased AGN activity is not related to cooling flows, but rather to accretion of gas-rich satellites at early times. These accretion events ought to throw off the precise cooling/feedback balance in the centers of clusters that responsible for preventing runaway cooling flows, which leads to a less tightly regulated feedback loop at early times. Further studies with deeper and higher angular resolution mid-IR imaging, such as the upcoming James Webb Space Telescope (JWST; Gardner et al. 2006), will be required to better understand the evolution of AGN feedback and its impact on galaxy clusters.

T.S. and M.M. acknowledge support from the Kavli Research Investment Fund at MIT, and from NASA through Chandra grant GO5-16143.

F.R. acknowledges financial support provided by NASA through SAO Award Number SV2-82023 issued by the Chandra X-Ray Observatory Center, which is operated by the Smithsonian Astrophysical Observatory for and on behalf of NASA under contract NAS8-03060.

This publication makes use of data products from the Wide-field Infrared Survey Explorer, which is a joint project of the University of California, Los Angeles, and the Jet Propulsion Laboratory/California Institute of Technology, funded by the National Aeronautics and Space Administration.

The South Pole Telescope is supported by the National Science Foundation through grant PLR-1248097. Partial support is also provided by the NSF Physics Frontier Center grant PHY-1125897 to the Kavli Institute of Cosmological

Physics at the University of Chicago, the Kavli Foundation, and the Gordon and Betty Moore Foundation grant GBMF 947.

Funding for the DES Projects has been provided by the U.S. Department of Energy, the U.S. National Science Foundation, the Ministry of Science and Education of Spain, the Science and Technology Facilities Council of the United Kingdom, the Higher Education Funding Council for England, the National Center for Supercomputing Applications at the University of Illinois at Urbana-Champaign, the Kavli Institute of Cosmological Physics at the University of Chicago, the Center for Cosmology and Astro-Particle Physics at the Ohio State University, the Mitchell Institute for Fundamental Physics and Astronomy at Texas A&M University, Financiadora de Estudos e Projetos, Fundação Carlos Chagas Filho de Amparo à Pesquisa do Estado do Rio de Janeiro, Conselho Nacional de Desenvolvimento Cientìfico e Tecnológico and the Ministério da Ciência, Tecnologia e Inovação, the Deutsche Forschungsgemeinschaft and the Collaborating Institutions in the Dark Energy Survey.

The Collaborating Institutions are Argonne National Laboratory, the University of California at Santa Cruz, the University of Cambridge, Centro de Investigaciones Enérgeticas, Medioambientales y Tecnológicas-Madrid, the University of Chicago, University College London, the DES-Brazil Consortium, the University of Edinburgh, the Eidgenössische Technische Hochschule (ETH) Zürich, Fermi National Accelerator Laboratory, the University of Illinois at Urbana-Champaign, the Institut de Ciències de l'Espai (IEEC/CSIC), the Institut de Fìsica d'Altes Energies, Lawrence Berkeley National Laboratory, the Ludwig-Maximilians-Universität München and the associated Excellence Cluster Universe, the University of Michigan, the National Optical Astronomy Observatory, the University of Nottingham, The Ohio State University, the OzDES Membership Consortium, the University of Pennsylvania, the University of Portsmouth, SLAC National Accelerator Laboratory, Stanford University, the University of Sussex, and Texas A&M University.

Facilities: Pan-STARRS, Chandra X-ray Observatory (ACIS), Hubble Space Telescope (ACS/WFC), the Nordic Optical Telescope (ALFOSC).

Software: astropy (Astropy Collaboration et al. 2018), CIAO (Fruscione et al. 2006), pandas (McKinney 2010), seaborn (Waskom et al. 2016).

ORCID iDs

T. Somboonpanyakul https://orcid.org/0000-0003-3521-3631
M. McDonald https://orcid.org/0000-0001-5226-8349
M. Aguena https://orcid.org/0000-0001-5679-6747
M. B. Bayliss https://orcid.org/0000-0003-1074-4807
E. Bertin https://orcid.org/0000-0002-3602-3664
D. Brooks https://orcid.org/0000-0002-8458-5047
D. L. Burke https://orcid.org/0000-0003-1866-1950
M. Calzadilla https://orcid.org/0000-0002-2238-2105
A. Carnero Rosell https://orcid.org/0000-0003-3044-5150
M. Carrasco Kind https://orcid.org/0000-0002-4802-3194
J. Carretero https://orcid.org/0000-0002-3130-0204
M. Costanzi https://orcid.org/0000-0001-8158-1449
L. N. da Costa https://orcid.org/0000-0002-7731-277X
J. De Vicente https://orcid.org/0000-0001-8318-6813
A. E. Evrard https://orcid.org/0000-0002-4876-956X
I. Ferrero https://orcid.org/0000-0002-1295-1132
B. Floyd https://orcid.org/0000-0003-4175-571X
J. García-Bellido https://orcid.org/0000-0002-9370-8360
E. Gaztanaga https://orcid.org/0000-0001-9632-0815
D. W. Gerdes https://orcid.org/0000-0001-6942-2736
A. Gonzalez https://orcid.org/0000-0002-0933-8601
D. Gruen https://orcid.org/0000-0003-3270-7644
R. A. Gruendl https://orcid.org/0000-0002-4588-6517
J. Gschwend https://orcid.org/0000-0003-3023-8362
N. Gupta https://orcid.org/0000-0001-7547-4241
S. R. Hinton https://orcid.org/0000-0003-2071-9349
D. L. Hollowood https://orcid.org/0000-0002-9369-4157
T. Jeltema https://orcid.org/0000-0001-6089-0365
G. Khullar https://orcid.org/0000-0002-3475-7648
K. J. Kim https://orcid.org/0000-0001-6505-0293
K. Kuehn https://orcid.org/0000-0003-0120-0808
J. L. Marshall https://orcid.org/0000-0003-0710-9474
P. Martini https://orcid.org/0000-0002-4279-4182
P. Melchior https://orcid.org/0000-0002-8873-5065
F. Menanteau https://orcid.org/0000-0002-1372-2534
R. Miquel https://orcid.org/0000-0002-6610-4836
R. Morgan https://orcid.org/0000-0002-7016-5471
R. L. C. Ogando https://orcid.org/0000-0003-2120-1154
A. Palmese https://orcid.org/0000-0002-6011-0530
F. Paz-Chinchón https://orcid.org/0000-0003-1339-2683
A. Pieres https://orcid.org/0000-0001-9186-6042
A. A. Plazas Malagón https://orcid.org/0000-0002-2598-0514
A. K. Romer https://orcid.org/0000-0002-9328-879X
F. Ruppin https://orcid.org/0000-0002-0955-8954
E. Sanchez https://orcid.org/0000-0002-9646-8198
S. Serrano https://orcid.org/0000-0002-0211-2861
I. Sevilla-Noarbe https://orcid.org/0000-0002-1831-1953
M. Smith https://orcid.org/0000-0002-3321-1432
M. Soares-Santos https://orcid.org/0000-0001-6082-8529
V. Strazzullo https://orcid.org/0000-0001-7975-2894
M. E. C. Swanson https://orcid.org/0000-0002-1488-8552
G. Tarle https://orcid.org/0000-0003-1704-0781
C. To https://orcid.org/0000-0001-7836-2261
D. L. Tucker https://orcid.org/0000-0001-7211-5729

References

Assef, R. J., Stern, D., Kochanek, C. S., et al. 2013, ApJ, 772, 26
Astropy Collaboration, Price-Whelan, A. M., Sipőcz, B. M., et al. 2018, AJ, 156, 123
Barnes, J. E., & Hernquist, L. E. 1991, ApJL, 370, L65
Bayliss, M. B., Ruel, J., Stubbs, C. W., et al. 2016, ApJS, 227, 3
Bîrzan, L., Rafferty, D. A., Brüggen, M., et al. 2017, MNRAS, 471, 1766
Bleem, L. E., Bocquet, S., Stalder, B., et al. 2020, ApJS, 247, 25
Bleem, L. E., Stalder, B., de Haan, T., et al. 2015, ApJS, 216, 27
Bocquet, S., Dietrich, J. P., Schrabback, T., et al. 2019, ApJ, 878, 55
Böhringer, H., Schuecker, P., Guzzo, L., et al. 2004, A&A, 425, 367
Bonaventura, N. R., Webb, T. M. A., Muzzin, A., et al. 2017, MNRAS, 469, 1259
Brammer, G. B., van Dokkum, P. G., & Coppi, P. 2008, ApJ, 686, 1503
Brown, L. D., Cai, T. T., & DasGupta, A. 2001, StaSc, 16, 101
Bruzual, G., & Charlot, S. 2003, MNRAS, 344, 1000
Carlstrom, J. E., Ade, P. A. R., Aird, K. A., et al. 2011, PASP, 123, 568
Chabrier, G. 2003, PASP, 115, 763
Churazov, E., Sazonov, S., Sunyaev, R., et al. 2005, MNRAS, 363, L91
Conroy, C., Gunn, J. E., & White, M. 2009, ApJ, 699, 486
Donahue, M., Connor, T., Fogarty, K., et al. 2015, ApJ, 805, 177
Dunne, D. A., Webb, T. M. A., Noble, A., et al. 2021, ApJL, 909, L29
Ebeling, H., Edge, A. C., Allen, S. W., et al. 2000, MNRAS, 318, 333
Ebeling, H., Edge, A. C., & Henry, J. P. 2001, ApJ, 553, 668
Ehlert, S., Allen, S. W., von der Linden, A., et al. 2011, MNRAS, 411, 1641
Eisenhardt, P. R. M., Marocco, F., Fowler, J. W., et al. 2020, ApJS, 247, 69

Fabian, A. C. 1994, ARA&A, 32, 277
Fabian, A. C. 2012, ARA&A, 50, 455
Fakhouri, O., Ma, C.-P., & Boylan-Kolchin, M. 2010, MNRAS, 406, 2267
Fazio, G. G., Hora, J. L., Allen, L. E., et al. 2004, ApJS, 154, 10
Fruscione, A., McDowell, J. C., Allen, G. E., et al. 2006, Proc. SPIE, 6270, 62701V
Gardner, J. P., Mather, J. C., Clampin, M., et al. 2006, SSRv, 123, 485
Gaspari, M., Tombesi, F., & Cappi, M. 2020, Nature Astronomy, 4, 10
Gunn, J. E., & Gott, J. R. I. 1972, ApJ, 176, 1
Gupta, N., Pannella, M., Mohr, J. J., et al. 2020, MNRAS, 494, 1705
Haggard, D., Green, P. J., Anderson, S. F., et al. 2010, ApJ, 723, 1447
Hasinger, G., Miyaji, T., & Schmidt, M. 2005, A&A, 441, 417
Hayashi, M., Tadaki, K., Kodama, T, et al. 2018, ApJ, 856, 118
Hickox, R. C., & Alexander, D. M. 2018, ARA&A, 56, 625
Hilton, M., Hasselfield, M., Sifón, C., et al. 2018, ApJS, 235, 20
Hilton, M., Sifón, C., Naess, S., et al. 2021, ApJS, 253, 3
Hlavacek-Larrondo, J., Allen, S. W., Taylor, G. B., et al. 2013, ApJ, 777, 163
Hlavacek-Larrondo, J., Fabian, A. C., Edge, A. C., et al. 2013, MNRAS, 431, 1638
Hlavacek-Larrondo, J., McDonald, M., Benson, B. A., et al. 2015, ApJ, 805, 35
Hopkins, P. F., Hernquist, L., Cox, T. J., et al. 2006, ApJS, 163, 1
Huang, N., Bleem, L. E., Stalder, B., et al. 2020, AJ, 159, 110
Jarvis, M., Bernstein, G. M., Amon, A., et al. 2021, MNRAS, 501, 1282
Khullar, G., Bleem, L. E., Bayliss, M. B., et al. 2019, ApJ, 870, 7
Kriek, M., van Dokkum, P. G., Labbé, I., et al. 2009, ApJ, 700, 221
Lacy, M., Storrie-Lombardi, L. J., Sajina, A., et al. 2004, ApJS, 154, 166
Lang, D. 2014, AJ, 147, 108
Larson, R. B., Tinsley, B. M., & Caldwell, C. N. 1980, ApJ, 237, 692
Lehmer, B. D., Brandt, W. N., Alexander, D. M., et al. 2007, ApJ, 657, 681
Mainzer, A., Bauer, J., Cutri, R. M., et al. 2014, ApJ, 792, 30
Mancone, C. L., & Gonzalez, A. H. 2012, PASP, 124, 606
Maraston, C. 2005, MNRAS, 362, 799
Markevitch, M., Gonzalez, A. H., Clowe, D., et al. 2004, ApJ, 606, 819
Markov, V., Mei, S., Salomé, P., et al. 2020, A&A, 641, A22
Martini, P., Sivakoff, G. R., & Mulchaey, J. S. 2009, ApJ, 701, 66
McDonald, M., Allen, S. W., Bayliss, M., et al. 2017, ApJ, 843, 28
McDonald, M., Benson, B. A., Vikhlinin, A., et al. 2013, ApJ, 774, 23
McDonald, M., Gaspari, M., McNamara, B. R., et al. 2018, ApJ, 858, 45
McDonald, M., McNamara, B. R., Calzadilla, M. S., et al. 2021, ApJ, 908, 85
McDonald, M., Stalder, B., Bayliss, M., et al. 2016, ApJ, 817, 86
McKinney, W. 2010, in Proc. IX Python in Science Conf., ed. S. van der Walt & J. Millman (Austin, TX: SciPy), 51
McNamara, B. R., & Nulsen, P. E. J. 2012, NJPh, 14, 055023
Merritt, D. 1983, ApJ, 264, 24
Mo, W., Gonzalez, A., Brodwin, M., et al. 2020, ApJ, 901, 131
Noble, A. G., McDonald, M., Muzzin, A., et al. 2017, ApJL, 842, L21
Noble, A. G., Muzzin, A., McDonald, M., et al. 2019, ApJ, 870, 56
O'Dea, C. P., Baum, S. A., Privon, G., et al. 2008, ApJ, 681, 1035
O'Sullivan, E., Giacintucci, S., Babul, A., et al. 2012, MNRAS, 424, 2971
Rafferty, D. A., McNamara, B. R., Nulsen, P. E. J., et al. 2006, ApJ, 652, 216
Ruppin, F., McDonald, M., Bleem, L. E., et al. 2021, ApJ, 918, 43
Russell, H. R., Fabian, A. C., Sanders, J. S., et al. 2010, MNRAS, 402, 1561
Russell, H. R., McNamara, B. R., Edge, A. C., et al. 2013, MNRAS, 432, 530
Salpeter, E. E. 1955, ApJ, 121, 161
Sarazin, C. L. 1986, RvMP, 58, 1
Sevilla-Noarbe, I., Bechtol, K., Carrasco Kind, M., et al. 2021, ApJS, 254, 24
Silverman, J. D., Green, P. J., Barkhouse, W. A., et al. 2008, ApJ, 679, 118
Silverman, J. D., Kovač, K., Knobel, C., et al. 2009, ApJ, 695, 171
Singal, J., George, J., & Gerber, A. 2016, ApJ, 831, 60
Somboonpanyakul, T., McDonald, M., Bayliss, M., et al. 2021b, ApJL, 907, L12
Somboonpanyakul, T., McDonald, M., Gaspari, M., et al. 2021a, ApJ, 910, 60
Stern, D., Assef, R. J., Benford, D. J., et al. 2012, ApJ, 753, 30
Stern, D., Djorgovski, S. G., Perley, R. A., et al. 2000, AJ, 119, 1526
Stern, D., Eisenhardt, P., Gorjian, V., et al. 2005, ApJ, 631, 163
Sunyaev, R. A., & Zeldovich, Y. B. 1972, A&A, 20, 189
Voit, G. M. 2005, RvMP, 77, 207
Voit, G. M. 2018, ApJ, 868, 102
Voit, G. M., Donahue, M., Bryan, G. L., et al. 2015, Natur, 519, 203
Waskom, M., Botvinnik, O., Drewokane, et al. 2016, Seaborn: v0.7.1, Zenodo, doi:10.5281/zenodo.54844
Webb, T. M. A., Muzzin, A., Noble, A., et al. 2015, ApJ, 814, 96
Wright, E. L., Eisenhardt, P. R. M., Mainzer, A. K., et al. 2010, AJ, 140, 1868
Yang, L., Tozzi, P., Yu, H., et al. 2018, ApJ, 859, 65
Zwicky, F. 1933, AcHPh, 6, 110